MICHIGAN STATE UNIVERSITY

CYCLOTRON LABORATORY

A FINITE RANGE-DWBA STUDY OF THE (^{4}He, ^{6}Li) REACTION ON ^{12}C, ^{24}Mg and ^{40}Ca

R.G. MARKHAM and M.A.M. SHAHABUDDIN

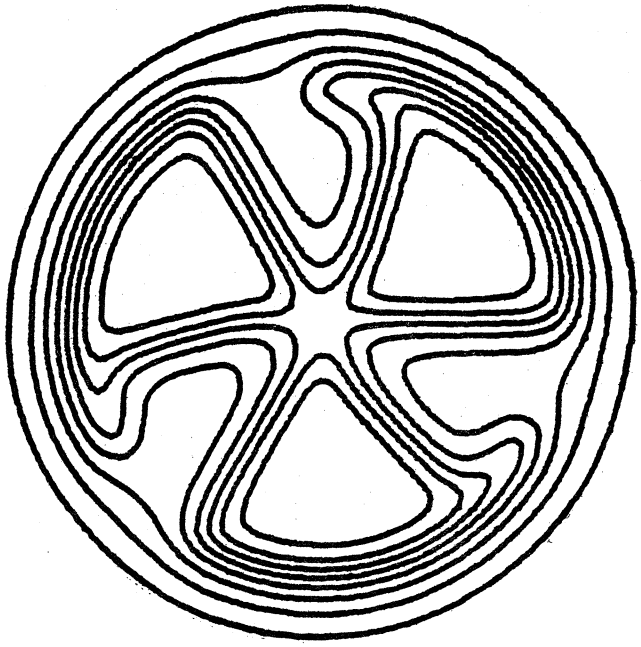

MSUCL-192 OCTOBER 1975

A Finite Range-DWBA Study of the (^{4}He,^{6}Li) Reaction on ^{12}C, ^{24}Mg and ^{40}Ca*

R.G. Markham and M.A.M. Shahabuddin

Cyclotron Laboratory and Physics Department
Michigan State University, East Lansing, Michigan 48824

ABSTRACT

Angular distributions have been obtained for the (α,^{6}Li) reaction at 46 MeV on targets of ^{12}C, ^{24}Mg and ^{40}Ca. A finite range DWBA analysis is performed using shell model wave functions to describe the target and various cluster wave functions to describe ^{6}Li. Reasonable agreement between measured and predicted absolute cross sections is obtained only if the product of the α-d wave function and potential for the ^{6}Li has no node. Finite range effects are important.

NUCLEAR REACTIONS: ^{12}C, ^{24}Mg, ^{40}Ca(α,^{6}Li), E=46 MeV; measured $\sigma(E_{Li},\theta)$: Finite-range DWBA analysis with microscopic wave functions.

*Work supported by the National Science Foundation.

I. INTRODUCTION

In recent years, there has been a great deal of interest in the (^{6}Li,d) "alpha" transfer reaction. Studies[1] have found that the angular distributions have shapes which are characteristic of the transferred L and reproducible with both finite range and zero range DWBA calculations. Thus, the reaction has been very useful for making spin assignments, but so far it has only been possible to discuss the relative cross sections. The significance of the absolute cross sections is completely unknown. The prediction of absolute cross sections based on shell model wave functions requires a microscopic four nucleon form factor and a reliable reaction theory. The difficulties inherent in the construction of such a form factor and the lack of knowledge of the structure of ^{6}Li (which is required in a finite range DWBA, FRDWBA, calculation) preclude a simultaneous solution to these problems. Thus, it is necessary to isolate the two problems and solve each independently. The (α,^{6}Li)--or (^{6}Li,α)--reaction allows one to make this separation since its analysis requires the same relative motion wave function and interaction potential of the alpha and deuteron in ^{6}Li but only a two nucleon form factor which is relatively well understood.

Very little data exists for either the (α,^{6}Li) or (^{6}Li,α) reactions. The very negative Q values (-15 to -25 MeV) for the (α,^{6}Li) reaction demand a high beam energy and so the few existing experiments[2] have been done on light nuclei with poor resolution. Tentatively it is concluded from these

works that the reaction is direct. The $^{20}Ne(^{6}Li,\alpha)^{22}Na$ reaction has been observed[3] with good resolution over a wide range of angles but no analysis has been performed.

Here we report a study of the $(\alpha,^{6}Li)$ reaction on targets of ^{12}C, ^{24}Mg and ^{40}Ca. Calculations are performed using FRDWBA with shell model form factors and two sets of ^{6}Li wave functions and potentials. The emphasis is on reproducing the absolute magnitudes of the cross sections to all states for which angular distributions have been obtained.

II. EXPERIMENT

The reactions were induced using 46 MeV alpha particles from the Michigan State University Cyclotron. Average beam intensities varied from 200 to 800 nA. The outgoing ^{6}Li ions were analyzed in a split pole spectrograph and detected in a dual proportional counter in the focal plane. The front counter was a single-wire, position-sensitive counter using charge division readout. The second counter was operated in coincidence and served to reduce background events due to the heavy ions (such as ^{12}C target recoils) which stopped in the front counter and produced pulses the same size as those of the ^{6}Li. Otherwise particle identification was solely by pulse height in the front counter. Because of angle dependent path length differences in the counter, this means of identification provided adequate separation only if the solid angle was limited to 2 msr.

The target thicknesses were 100±10, 52±10, and 371±80 $\mu g/cm^2$ for ^{12}C, ^{24}Mg, and ^{40}Ca respectively. These thicknesses were determined by alpha gauge measurements for ^{12}C, comparison of elastic scattering yields with thicker, known foils for ^{24}Mg and energy loss measurements using the outgoing ^{6}Li for the ^{40}Ca target. In the last case, the reaction peaks were flat topped with width determined by the target thickness and orientation. The widths of the lines were studied as a function of target angle, and the target thickness was then deduced using the known stopping powers of ^{6}Li and ^{4}He. Absolute cross sections were computed from integrated charge and the above target thicknesses; relative yields at the various angles were fixed in relation to a monitor detector at 60°.

Angular distributions were taken from 11° to 60° center of mass in the ^{12}C experiment with the largest angle determined by the very low energy of the outgoing ^{6}Li. (For this reaction the ground-state Q-value is -23.7 MeV.) The decrease of cross section with angle limited the angular range to less than 80° and 55° for ^{24}Mg and ^{40}Ca respectively.

Typical spectra are shown in Fig. 1. The energy resolution in all cases was target thickness limited but adequate to resolve the low lying T=0 states. There is no evidence for population of any of the low lying $J^{\pi}=0^{+}$, T=1 states at 1.740, 0.656, and 0.132 MeV in ^{10}B, and ^{22}Na and ^{38}K respectively.

The angular distributions are shown in Fig. 2. They are most forward peaked for the ^{40}Ca target where they fall off

an order of magntidue from 11° to 55° and become successively less forward peaked for the lighter targets. An additional measurement was taken at 120° CM on the ^{24}Mg target. The cross sections for all the states were lower by factors of 2 to 10 than the cross sections at 60° thus indicating a lack of symmetry about 90°.

III. FRDWBA ANALYSIS

Calculations using the finite range DWBA code "LOLA"[4] have been carried out. As mentioned in the introduction such a treatment of the reaction requires a knowledge of the relative motion wave function $\psi_{\alpha d}$ of the alpha and deuteron in ^{6}Li and the interaction potential $v_{\alpha d}$. We have tried two sets of wave functions and potentials. The first, to be referred to as Li1, is the Eckart function and potential with the parameters determined by Nobel[5] (ϵ=0, R=1.5 fm). This function has only one node, at zero separation. The potential has a repulsive core (necessary to produce the node at the origin) which may be thought of as a manifestation of the Pauli principle. The parameters of the wave function have been derived from elastic electron scattering data and static M1 and E2 moments. Further, it reproduces momentum distributions obtained from ^{6}Li(p,pα), ^{6}Li(α,2α), and ^{6}Li(p,pd) reactions and has the proper vertex constant as concluded by Lim.[6] However, there are functions (2S Harmonic Oscillator) that have a node away from the origin that fit these same data equally well. Thus, we can not be sure that $\psi_{\alpha d}$, much less the product, $\psi_{\alpha d}$ $V_{\alpha d}$ has the correct form. Despite the large differences between this wave function

and the 2S radial form commonly used, the products $\psi_{\alpha d}$ $V_{\alpha d}$ have a similar form and should lead to similar results in a FRDWBA calculation.

Thus, we arbitrarily chose a very different form for the second wave function and potential (Li2) tried. The radial wave function is similar to the Eckart function and the potential is purely attractive with a Woods-Saxon shape. The justification for such a choice is that the Eckart function is a reasonable choice for an antisymmetrized relative motion wave function because of the suppressed probability for both the deuteron and the alpha being at the same place and a purely attractive potential is not unreasonable. As mentioned before the node at the origin requires a repulsive core potential; thus a Woods-Saxon well will not generate the desired radial shape (for an L=0 state of relative motion). Here we assume that the Woods-Saxon well generates a radial wave function that after antisymmetrization of the total ^{6}Li wave function has the desired shape. This is in marked contrast to the possible points of view when using the Eckart function and potential which are: that the potential generates an antisymmetric form because it contains the proper exchange terms (repulsive core), or that the repulsive core is not due to the Pauli Principle and that antisymmetrization of the resulting wave function does not have a significant effect.

The Li2 wave function was calculated as a bound state of a Woods-Saxon potential with a repulsive core added. This repulsive core was not used in the finite range calculations; thus, the product $\psi_{\alpha d}$ $V_{\alpha d}$ had its node at the origin. The form of the

repulsive core was, somewhat arbitrarily chosen, to be equivalent to the centrifugal potential for L=2 (as done by Gutbrod[7]) and the parameters of the well (equivalent to those used by DeVries[1]) were chosen to produce a radial shape similar to that of the Eckart function and most nearly like that used by Jain.[8]

The target form factors were generated microscopically from single-particle wave functions according to the technique of Bayman and Kallio.[9] The protons and neutrons were bound in the same potential well with the sum of the proton and neutron binding energies equal to the deuteron separation energy. The two nucleon parentage amplitudes for the ^{40}Ca and ^{24}Mg experiments were taken from two different sets of shell model wave functions.[10,11,12,13] For the ^{12}C experiment, the wave functions of Cohen-and Kurath[14] were used.

Many optical model parameters were tried with greatly varing degrees of success. The sets we found most suitable are listed in Table I. The criteria for whether a set of parameters was acceptable or not was the fit to the shapes of the angular distributions.

IV. THE ANGULAR DISTRIBUTIONS

The results of the finite range calculations using Li2 for the ^{6}Li wave function and potential and using shell model form factors are shown in Fig. 2. The curves are the sum of the allowed L transfers and each curve is independently normalized to the data. In all but one case, the theoretical curves are dominated by a single L transfer; for that case, the most significant contributing L is also plotted. The factors

needed to normalize the theory to the data are listed in Table II; ideally, they should be about equal to one. The calculations using Lil for the ^{6}Li wave function and potential gave very similar angular distributions and so are not shown. However, the absolute magnitudes are very different for the two calculations.

A. The ^{40}Ca(α, ^{6}Li)^{38}K Reaction

Two sets of shell model wave functions for ^{38}K were tried. In both cases, ^{40}Ca was taken as the closed core so the ^{38}K wave functions differ only in the choice of two body interaction. The predicted cross sections are the same within thirty percent and the angular distributions are little affected.

The ground state is populated by an almost pure L=4 transfer. The shape of the angular distribution is rather well reproduced but the theory predicts too many small oscillations. This is more apparent for the first excited $J^{\pi}=1^{+}$ state which is populated by a mixture of L=0 and 2. No combination of these L transfers can remove the oscillations implying that the problem is due to the choice of parameters for the optical model or bound states.

The measured angular distribution for the second excited $J^{\pi}=1^{+}$ state is very similar to the one for the first excited state. The shell model predicts it to be excited by an almost pure L=0 transfer, but this apparently is not the case. Furthermore the cross sections for both $J^{\pi}=1^{+}$ states are relatively underpredicted compared to the ground state. Thus, we feel that

the shell model is the source of difficulty here and in particular the difficulty may be related to the assumed shell closure at ^{40}Ca.

B. The $^{24}Mg(\alpha,^{6}Li)^{22}Na$ Reaction

Two sets of shell model wave functions for ^{24}Mg and ^{22}Na were tried. The first set was constructed in a truncated model space and the second in the full s-d shell. Again both sets gave similar angular distributions (only the predictions using the full space are shown in Fig. 2).

Again the ground state angular distribution is well reproduced, but in this case the transfer is almost pure L=2 in character. The first excited $J^{\pi}=1^{+}$ state is poorly fitted by the predicted L=0 transfer. The shape of the $J^{\pi}=1^{+}$ angular distribution strongly resembles the ground state L=2 shape and so we feel it is largely populated by L=2. Both sets of shell model wave functions predict the dominance of the L=0 component, but this transition is the most sensitive to the change of model space.

The $J^{\pi}=4^{+}$ and 5^{+} states can only be populated by L=4 transfer. The shapes of the angular distributions are well reproduced particularly for the $J^{\pi}=5^{+}$ state. However, the cross sections are under-predicted by large factors. Both transitions are quite sensitive to the choice of shell model wave functions, but because of the size of the discrepancy, the prospect that additional reaction channels are important must be considered.

C. The $^{12}C(\alpha,^{6}Li)^{10}B$ Reaction

The shell model wave functions of Cohen and Kurath[14] were used to describe the states of ^{10}B and ^{12}C. The ground state angular distribution is fit very well by the predicted L=2 angular distribution. The fits to the first and second excited $J^{\pi}=1^{+}$ states are less satisfactory with the predicted angular distributions becoming too flat with increased excitation energy. In this instance, both $J^{\pi}=1^{+}$ states are dominated by L=0 transfers.

The $J^{\pi}=2^{+}$ state at 3.59 MeV is seen only weakly and has a rather structureless angular distribution. The predicted L=2 angular distribution, also rather flat, seems to be out of phase with the data. The energy in the center of mass is quite low in the outgoing channel for these excited states so it is to be expected that an energy independent optical model will not reproduce the Q-value dependence of the reaction.

V. ABSOLUTE CROSS SECTIONS

In general, the agreement between theory and experiment is very good when the Li2 wave function and potential is used. If we ignore the $J^{\pi}=4^{+}$ and 5^{+} states of ^{22}Na, we find that the ratio of experimental to theoretical cross sections varies from 0.3 to 4.2 for Li2 and from 6 to 291 for Li1. Not only are these ratios much closer to unity for Li2; but also, they are more nearly constant. The ratio of Li2 to Li1 cross sections for all states are tabulated in the last column of Table II. These ratios show that the Li1 cross sections are both

considerably smaller (factors of 18 to 68) and not simply related to the Li2 cross sections as would be expected if the zero-range approximation were valid (the ratio of D_o^2 for Li2 to D_o^2 for Li1 is 16.5).

A probable explanation is that the presence of a node in the product of the wave function and potential for Li1 makes it possible for the positive and negative portions of the product to give canceling contributions to the DWBA integral. The degree of cancellation will clearly depend on the position of the node, on the shape of the wave function and potential and on all of the other parameters of the calculation. A demonstration of the dependence of the cross section on the node position is shown in Fig. 3. This figure shows the relative zero degree cross sections for the L=0 contribution to the first $J^\pi=1^+$ state of ^{38}K as a function of node position (and well radius parameter). The wave functions and potentials were obtained by searching on the well depths of Woods-Saxon wells of various radii to produce 2S radial wave functions of the proper binding energy. Notice there is a very localized and dramatic decrease of the cross section near a node position of 2 fm. If the node is taken at very large radii (>3 fm), the cross section increases to somewhat less than the Li2 cross section. Likewise the cross sections become more near agreement with experiment for node positions close to zero but for this 2S form the Woods-Saxon well must have an unphysically small radius.

From this we conclude that the product of the ^6Li wave function and potential is unlikely to have a node except

possibly at zero separation. A similar conclusion was reached by Gutbrod et al.[7] in an analysis of the $(d,^6Li)$ reaction of p and s-d shell targets. They observed that the 2S radial form with a Woods-Saxon well vastly over estimated the decrease of cross section with increasing target mass. We do not observe this same phenomenon, but such an effect would be sensitive to the other details of the reaction.

VI. SUMMARY

The $(\alpha,^6Li)$ reaction seems to proceed via a simple direct mechanism with the angular distributions being forward peaked and isospin being conserved. However, the $J^\pi=4^+$ and 5^+ states in ^{22}Na are populated with anomalously large cross sections which suggests the possible importance of other reaction channels.

The shapes of the angular distributions were sensitive to the optical model parameters and insensitive to the choice of ^6Li wave function or interaction. The quality of the fits varied greatly depending most on the ability of the shell model to predict the proper ratio of L-transfers. The most difficulty was encountered with $J^\pi=1^+$ states. The predicted absolute magnitudes were found to be very sensitive to the ^6Li wave function and potential. This sensitivity was traced to cancellations in the integration caused by the presence of a node at r>0 in the product $V_{\alpha d}\,\psi_{\alpha d}$. Comparison to the data strongly supports the placement of the node at zero separation. With such a wave function and potential the absolute cross sections are well reproduced.

Based on these results we feel confident that if a proper four nucleon form factor could be constructed one would be able to predict absolute cross sections obtained in (^{6}Li,d) experiments. Further, the need for an exact finite range treatment is apparent if absolute magnitudes are to be calculated.

REFERENCES

1. H.W. Fulbright, U. Strohbusch, R.G. Markham, R.A. Lindgren, G.C. Morrison, S.C. McGuire and C.L. Bennett, Phys. Lett. 53B, 449(1975).
   R.M. DeVries, H.W. Fulbright, R.G. Markham and U. Strohbusch, Phys. Lett. 55B, 33(1975).
2. C.D. ZaFiratos, Phys. Rev. 136B, 1279(1964).
   P.F. Mizera and J.B. Gerhart, Phys. Rev. 170, 839(1968),
   B. Zeidman, H.T. Fortune and A. Ricter, Phys. Rev. C2, 1612(1970).
3. J.D. Garrett, R. Middleton, D.J. Pullen, S.A. Andersen, O. Nathan and O. Hansen, Nucl. Phys. A164, 449(1971).
4. R.M. DeVries, Phys. Rev. C8, 951(1973).
5. J.V. Noble, Phys. Rev. C9, 1209(1974).
6 T.K. Lim, Phys. Lett. 56B, 321(1975).
7. H.H. Gutbrod, H. Yoshida and R. Bock, Nucl. Phys. A165, 240(1971).
8. A.K. Jain, J.Y. Grossiord, M. Chevallier, P. Gaillard, A. Guichard, M. Gusakow, and J.R. Pizzi, Nucl. Phys. A216, 519(1973).
9. B.F. Bayman and A. Kallio, Phys. Rev. 156, 1121(1967).
10. B.H. Wildenthal, E.C. Halbert, J.B. McGrory and T.T.S. Kuo, Phys. Rev. C4, 1266(1971).
11. B.M. Preedom and B.H. Wildenthal, Phys. Rev. C6, 1633(1972), J.B. McGrory and B.H. Wildenthal, Phys. Lett. 34B, 373(1971).
12. B.H. Wildenthal and W. Chung, to be published.
13. B.H. Wildenthal and W. Chung, to be published.

TABLE I: Optical Model Parameters[a]

PART.	V_R	r_R^b	a_R	W_V	W_D	r_I^b	a_I	r_C^b	ref.
$^{40}Ca(^4He,^6Li)^{38}K$									
^4He	162.8	1.39	0.593	20.8	----	1.54	0.589	1.25	15
^6Li	250.0	1.40	0.65	0	25.0	1.4	0.65	1.4	16
p,n	48.0	1.25	0.65	----	-----	----	----	1.25	
$^{24}Mg(^4He,^6Li)^{22}Na$									
^4He	146.7	1.45	0.577	13.8	-----	1.45	0.577	1.25	17
^6Li	262.0	1.20	0.71	16.0	-----	1.75	1.15	1.4	18
p,n	62.9	1.25	0.65	----	-----	----	----	1.25	
$^{12}C(^4He,^6Li)^{10}B$									
^4He	151.9	1.24	0.665	28.5	-----	1.24	0.64	1.25	19
^6Li	232.0	1.25	0.755	----	6.03	2.34	0.56	2.5	20
p,n	56.9	1.25	0.65	----	-----	----	----	1.25	
^6Li bound state - Li2									
α-d	39.92	1.1	0.65	----	-----	----	----	1.25	$R=r(4^{1/3}+2^{1/3})$ $E_{\alpha d}$=-1.47 MeV

a) Units are MeV and fm

b) $R = r\ A_T^{1/3}$ fm except as noted

14. S. Cohen and D. Kurath, Nucl. Phys. A101, 1(1967).
15. D.F. Jackson and C.G. Morgan, Phys. Rev. 175, 1402(1968).
16. U. Strohbusch, private communication.
17. L. McFadden and G.R. Satchler, Nucl. Phys. 84, 177(1966).
18. V.I. Chuev, V.V. Davidov, B.G. Navatskii, A.A. Ogloblin, S.B. Sakuta and D.N. Stepanov, Jounal de Physique C6, 157(1971).
19. P. Gaillard, R. Bouche, L. Feuvrais, M. Gaillard, A. Guichard, M. Gusakow, J.L. Leonhardt and J.R. Pizzi, Nucl. Phys. A131, 353(1969).
20. J.W. Watson, Nucl. Phys. A198, 129(1972).

TABLE II: Ratios of Experimental to Theoretical Cross Sections

Target	J^π	Ex	Experiment/Theory Li2[a]	Li2[b]	Li1[b]	Ratio[c]
^{40}Ca	3^+	0.	0.75	0.74	28.	38.
	1^+	0.46	2.04	1.54	49.	32.
	1^+	1.70	1.83	2.17	44.	20.
^{24}Mg	3^+	0.	4.36	4.25	291.	68.
	1^+	0.58	7.71	4.24	254.	60.
	4^+	0.89	153	71.	4417.	62.
	5^+	1.53	14	19	1239.	65.
^{12}C	3^+	0.		0.89	18.	20.
	1^+	0.72		0.30	6.	20.
	1^+	2.15		0.63	13.	21.
	2^+	3.58		1.70	30.	18.

a) The shell model wave functions used are from Ref. 10 for ^{38}K and Ref. 11 for ^{22}Na and ^{24}Mg.

b) The shell model wave functions used are from Ref. 12 for ^{38}K, from Ref. 13 for ^{22}Na and ^{24}Mg and from Ref. 14 for ^{10}B and ^{12}C.

c) Ratio of column 6 to column 5. The ratio $D_o^2(Li2)/D_o^2(Li1) = 16.5$.

FIGURE CAPTIONS

Fig. 1--Typical spectra for the three reactions studied.

Fig. 2--Angular distributions for the three reactions. The statistical error bars (not shown) are approximately the size of the points being somewhat smaller for higher cross sections and somewhat larger for low cross sections. The curves are the result of finite range calculations. The dashed curve is the L=2 contribution.

Fig. 3--Relative zero degree cross sections for the L=0 component of the first $J^\pi=1^+$ state of ^{38}K plotted as a function of node position. For these calculations, a 2S solution of a Woods-Saxon well was used. The binding energy was held fixed at 1.47 MeV and the geometry was $a_r=0.65$, $R_c=R_R=r_o(4^{1/3} + 2^{1/3})$ with r_o varied from 0.1 to 3.0 fm. The line serves only to connect the calculated points. The corresponding magnitudes for Li1 and Li2 are indicated.

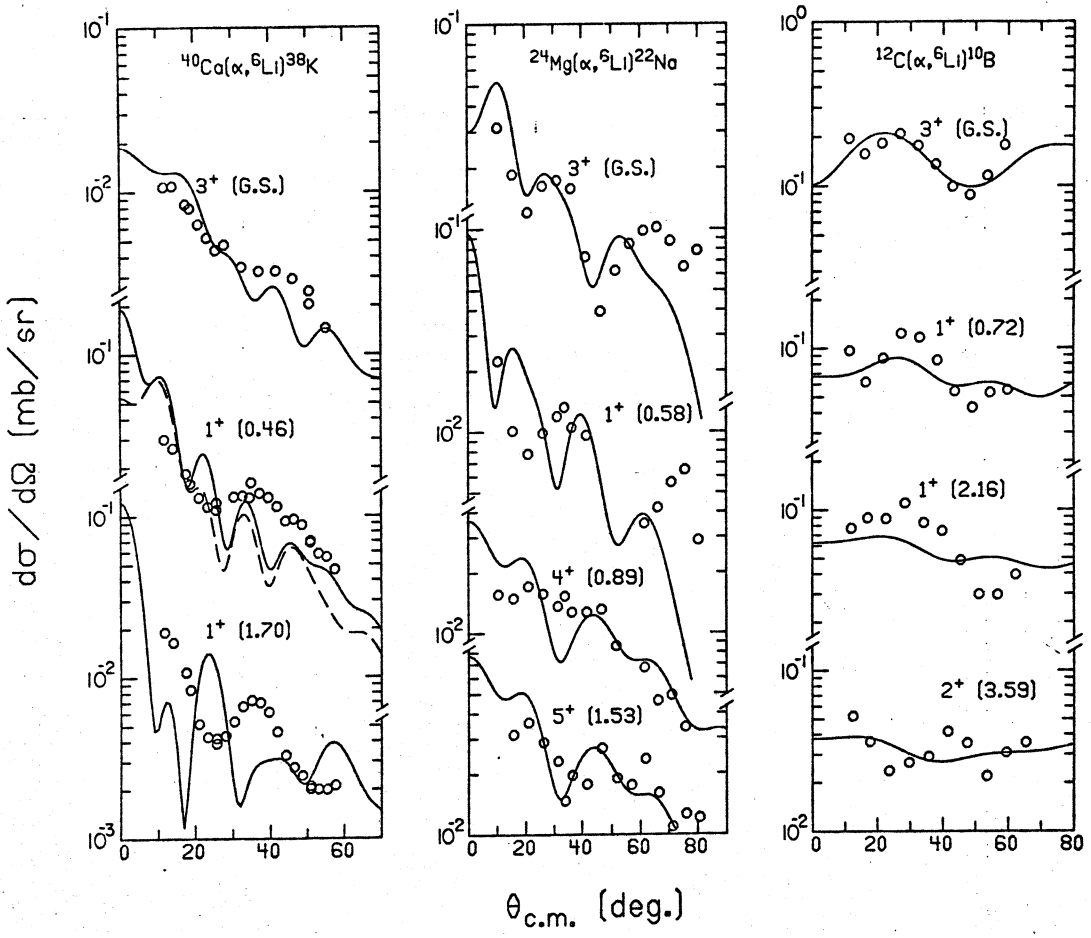
$^{40}Ca(\alpha,^6Li)^{38}K$
3+ (G.S.)
1+ (0.46)
1+ (1.70)
$^{24}Mg(\alpha,^6Li)^{22}Na$
3+ (G.S.)
1+ (0.58)
4+ (0.89)
5+ (1.53)
$^{12}C(\alpha,^6Li)^{10}B$
3+ (G.S.)
1+ (0.72)
1+ (2.16)
2+ (3.59)
$d\sigma/d\Omega$ (mb/sr)
$\theta_{c.m.}$ (deg.)

20

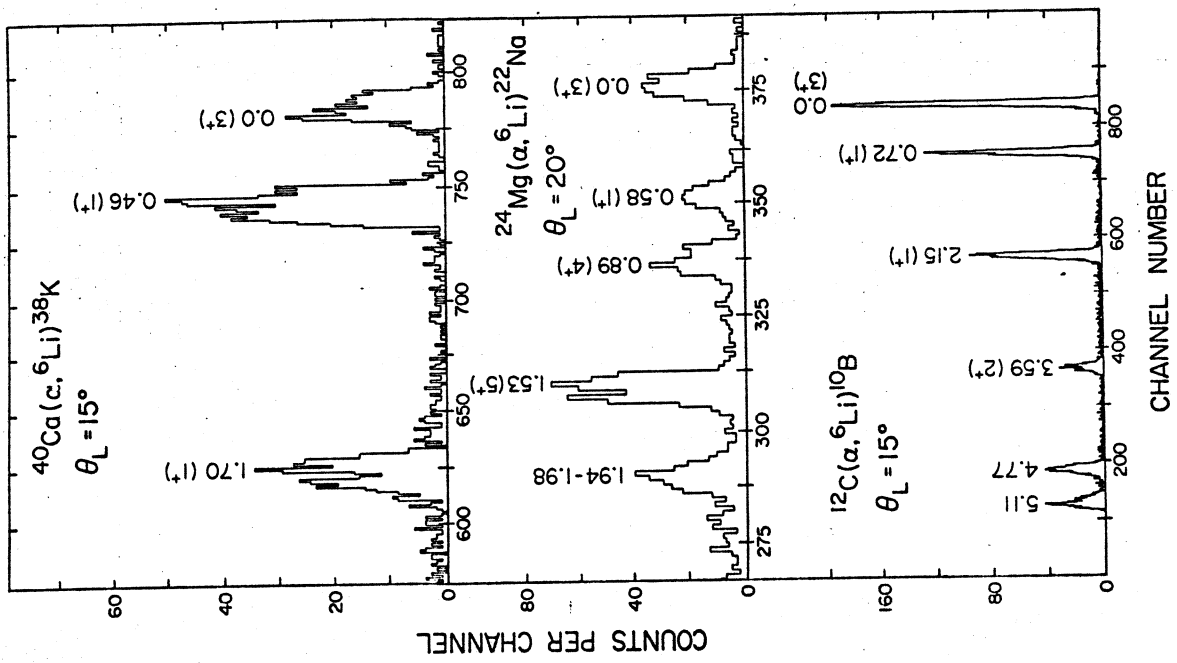
$^{40}Ca(c,^6Li)^{38}K$
$\theta_L = 15°$
0.0 (3+)
0.46 (1+)
1.70 (1+)
$^{24}Mg(\alpha,^6Li)^{22}Na$
$\theta_L = 20°$
0.0 (3+)
0.58 (1+)
0.89 (4+)
1.53 (5+)
1.94-1.98
$^{12}C(\alpha,^6Li)^{10}B$
$\theta_L = 15°$
0.0 (3+)
0.72 (1+)
2.15 (1+)
3.59 (2+)
4.77
5.11
COUNTS PER CHANNEL
CHANNEL NUMBER

19

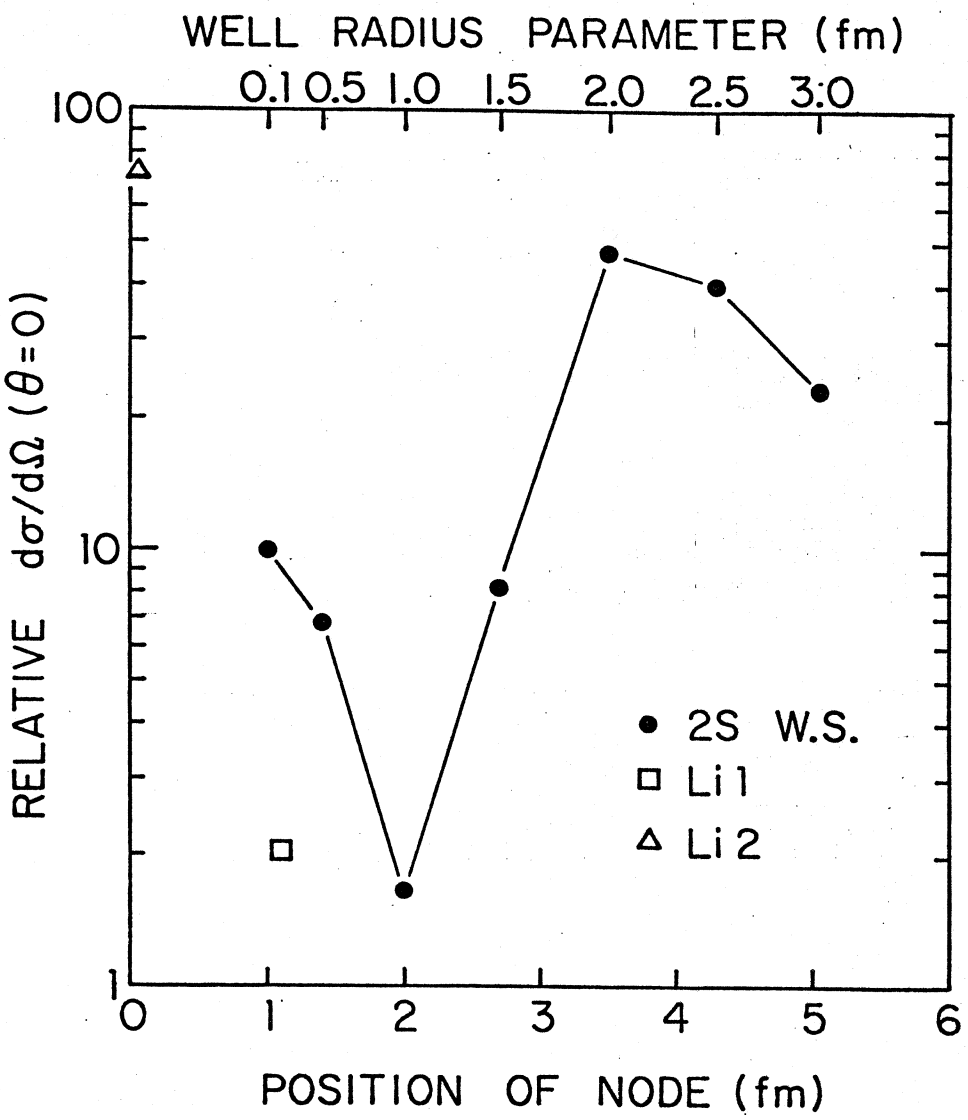
WELL RADIUS PARAMETER (fm)
0.1 0.5 1.0 1.5 2.0 2.5 3.0
100
10
1
RELATIVE dσ/dΩ (θ=0)
0 1 2 3 4 5 6
POSITION OF NODE (fm)
2S W.S.
Li 1
Li 2